

## Research Article

Theme: Translational Application of Nano Delivery Systems: Emerging Cancer Therapy  
Guest Editors: Mahavir B. Chougule and Chalet Tan

# Temperature-Tunable Iron Oxide Nanoparticles for Remote-Controlled Drug Release

Raj K. Dani,<sup>1</sup> Canan Schumann,<sup>1</sup> Olena Taratula,<sup>1,2</sup> and Oleh Taratula<sup>1,2</sup>

Received 11 December 2013; accepted 10 April 2014; published online 13 May 2014

**Abstract.** Herein, we report the successful development of a novel nanosystem capable of an efficient delivery and temperature-triggered drug release specifically aimed at cancer. The water-soluble  $130.1 \pm 0.2$  nm iron oxide nanoparticles (IONPs) were obtained *via* synthesis of a monodispersed iron oxide core stabilized with tetramethylammonium hydroxide pentahydrate (TMAOH), followed by coating with the thermoresponsive copolymer poly-(NIPAM-stat-AAm)-block-PEI (PNAP). The PNAP layer on the surface of the IONP undergoes reversible temperature-dependent structural changes from a swollen to a collapsed state resulting in the controlled release of anticancer drugs loaded in the delivery vehicle. We demonstrated that the phase transition temperature of the prepared copolymer can be precisely tuned to the desired value in the range of 36°C–44°C by changing the monomers ratio during the preparation of the nanoparticles. Evidence of modification of the IONPs with the thermoresponsive copolymer is proven by ATR-FTIR and a quantitative analysis of the polymeric and iron oxide content obtained by thermogravimetric analysis. When loaded with doxorubicin (DOX), the IONPs-PNAP revealed a triggered drug release at a temperature that is a few degrees higher than the phase transition temperature of a copolymer. Furthermore, an *in vitro* study demonstrated an efficient internalization of the nanoparticles into the cancer cells and showed that the drug-free IONPs-PNAP were nontoxic toward the cells. In contrast, sufficient therapeutic effect was observed for the DOX-loaded nanosystem as a function of temperature. Thus, the developed temperature-tunable IONPs-based delivery system showed high potential for remotely triggered drug delivery and the eradication of cancer cells.

**KEY WORDS:** drug delivery; IONPs; remote-triggered drug release; thermoresponsive copolymer; tunable LCST.

## INTRODUCTION

Recently, stimuli-responsive drug delivery systems introduced a promising tactic to precisely control drug delivery to the desired location (1). These systems experience rapid reversible changes in their structure triggered by external stimuli or small changes in the environment, proposing controlled drug release. Among other stimuli-responsive systems, temperature-responsive nanomaterials offer exciting new opportunities for controlled release of anticancer agents, specifically into the cancer cells, while diminishing severe side effects on the healthy organs (2,3). Thus, externally applied temperature could trigger the release of active agents from such

nanomaterials offering to control the required concentration or the release pattern of drugs at the targeted site (4). Special attention has been devoted to the thermoresponsive polymers, which respond to the temperature change by altering their physical, chemical, and colloidal properties and exhibiting a phase transition temperature, known as the lower critical solution temperature (LCST) (5,6). Aqueous solution of thermoresponsive polymer undergoes fast and reversible structural changes from a swollen to a collapsed state resulting in homogenous solution below the LCST and a phase separation above the LCST, which causes the on-off dissociation of drug molecules as a function of temperature (7).

If the temperature-responsive behavior can be combined with magnetic nanoparticles (8), which are able to generate heat in the presence of alternating magnetic field, this could be used to stimulate the temperature-sensitive polymer to release the drug locally at the targeted sites (9). For the magnetic performance, iron oxide nanoparticles (IONPs) have received great attention due to their applications ranging from MRI contrast agents, hyperthermia therapy, and image-guided drug delivery (10). The combination of the properties of IONPs and thermoresponsive polymer offers the remote-

**Electronic supplementary material** The online version of this article (doi:10.1208/s12249-014-0131-x) contains supplementary material, which is available to authorized users.

<sup>1</sup>Department of Pharmaceutical Sciences, College of Pharmacy, Oregon State University, 1601 SW Jefferson Street, Corvallis, Oregon 97331, USA.

<sup>2</sup>To whom correspondence should be addressed. (e-mail: olena.taratula@oregonstate.edu; olena.taratula@oregonstate.edu)

triggered drug release while reducing the toxic effects of the drug. Poly(*N*-isopropylacrylamide) (PNIPAM) has been extensively studied as a thermoresponsive polymer with the LCST around 32°C (11). However, the LCST of the PNIPAM polymer is below the physiological temperature which limits the drug delivery application of these polymers as the drug is released as soon as it is injected into the blood stream, preventing delivery to the targeted sites. Recently, it was shown that the LCST of PNIPAM could be controlled by including hydrophilic units (to increase the LCST) or hydrophobic residues (to lower the LCST) (12,13). Thus, Richard *et al.* (14) have studied the tunability of LCST of poly (2-oxazoline)s by varying its composition and molecular weight. Moreover, Zintchenko *et al.* (15) succeeded in the tuning of LCST in the range of 37°C–42°C of temperature-responsive polymers by using the copolymer polyethylenimine (PEI) as a cationic block and statistical copolymer of PNIPAM with the use of acrylamide (AAM) or vinylpyrrolidinone (VP) as a hydrophilic monomer.

To date, there are limited numbers of reports on the preparation of thermoresponsive magnetic nanoparticles with little efforts to tune the LCST of the nanoparticles that mainly involves coating with the PNIPAM-based polymers (16–21), encapsulation into polymeric micelles (22), and modification with biodegradable cellulose (23). If it is possible to control the LCST of water-soluble nanomaterials so that the LCST is a few degrees greater than body temperature, then such systems can be effectively utilized for the drug-controlled release systems.

Herein, we successfully employed a two-step approach for the synthesis of PNIPAM-based temperature-sensitive polymer-coated magnetic nanoparticles with tunable LCST aimed for use in the drug delivery for temperature-controlled drug release. For this work, the choice of the thermoresponsive shell, poly-(NIPAM-stat-AAM)-block-PEI (PNAP), is dictated by the biocompatibility profile of the polymer that has an LCST slightly higher than the body temperature. Due to the presence of the polymer shell, each individual nanoparticle can be efficiently loaded with the anticancer drug, doxorubicin (DOX) (Fig. 1). The valuable properties of the IONPs-PNAP as a new drug delivery system such as nanoparticle size and stability, LCST, drug loading efficiency, *in vitro* drug release, and cytotoxicity were evaluated. This system has shown to possess the desired properties to become a good candidate for an effective drug delivery vehicle with remote-controlled drug release. To the best

of our knowledge, no studies have been reported elsewhere that achieve the temperature-responsive polymer-coated iron oxide nanoparticles with tunable LCST.

## MATERIALS AND METHODS

### Materials

Ferrous chloride tetrahydrate ( $\text{FeCl}_2 \cdot 4\text{H}_2\text{O}$ ), ferric chloride hexahydrate ( $\text{FeCl}_3 \cdot 6\text{H}_2\text{O}$ ), and sodium hydroxide (NaOH) were purchased from AlfaAesar (Ward Hill, MA). *N*-isopropylacrylamide (NIPAM) was obtained from TCI (Japan). Ammonium persulfate (APS) and mercaptoethane (ME) were purchased from Amresco. Doxorubicin hydrochloride (DOX) was obtained from Polymed Therapeutics (Houston, TX). Branched polyethylenimine (PEI) (MW~25 kDa) and tetramethylammonium hydroxide pentahydrate (TMAOH) and acrylamide (AAM) were purchased from Sigma-Aldrich. Trinitrobenzene sulfonic acid (TNBSA) and bichinchonic acid (BCA) protein assay kits were obtained from Pierce (Rockford, IL). All chemicals were used without further purification except NIPAM which was twice recrystallized from hexane.

### Preparation of Iron Oxide Nanoparticles Coated with Thermoresponsive Copolymer

#### Stabilized Iron Oxide Nanoparticles

The iron oxide nanoparticles were prepared by an aqueous coprecipitation method following a previously published procedure by Lyon *et al.* (24) with some modifications. In brief, 1.99 g (10.0 mmol) of  $\text{FeCl}_2 \cdot 4\text{H}_2\text{O}$  and 5.40 g (20.0 mmol) of  $\text{FeCl}_3 \cdot 6\text{H}_2\text{O}$  were dissolved in 25 mL of Milli-Q water containing 315  $\mu\text{L}$  of conc. HCl. The solution was added dropwise into 250 mL of 1.5 M NaOH solution with vigorous stirring at 1,500 rpm (hotplate/stirrer, VWR) at room temperature (rt). The reaction mixture was stirred for 1 h. The resulting dark brown precipitate was isolated *via* magnetic decantation method and was washed with Milli-Q water twice. The final precipitate of nanoparticles was washed with 0.1 M tetramethylammonium hydroxide pentahydrate (TMAOH) solution and dispersed in 150 mL of 0.1 M TMAOH solution, resulting in the final iron oxide solution to be used for further modifications.

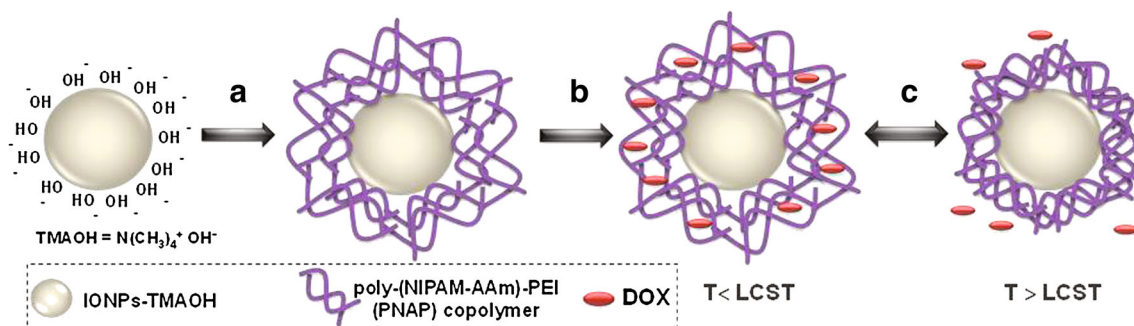


**Fig. 1.** Schematic representation of the development of the iron oxide nanoparticle (IONPs)-based nanocarrier for delivery of the anticancer drug and the temperature-triggered drug release process. **a** Modification of IONPs surface with a thermosensitive copolymer (PNAP). **b** Loading of anticancer agent (DOX) into the polymer reservoir on the surface of the IONPs. **c** Temperature-triggered drug release due to expansion/collapse of a copolymer chain on the surface of the IONPs depending on LCST of the poly-(NIPAM-AAM)-PEI copolymer

*Thermoresponsive Copolymer Poly-(NIPAM-stat-AAm)-Block-PEI (PNAP)*

The synthesis of the copolymer was carried out at rt following the previously published procedure by Zintchenko *et al.* (15) through radical copolymerization of NIPAM with AAm in water using APS as initiator in the presence of branched PEI. For synthesis of the copolymer with the NIPAM to AAm ratio of 3:1, 1.02 g (9.02 mmol) of NIPAM and 0.213 g (3.01 mmol) of AAm were dissolved in 10 mL of Milli-Q water; 0.50 g (~0.02 mmol) of PEI was dissolved in 5 mL of Milli-Q water and added to the resulting solution of NIPAM and AAm. Next, 17.5  $\mu$ L of ME was added to the reaction mixture to avoid the cross-linking due to the recombination of radicals. The reaction mixture was deoxygenated by bubbling nitrogen gas through it for 45 min to ensure optimum deoxygenation 0.011 g (0.046 mmol) of APS in 2 mL of Milli-Q water was injected into the reaction mixture to initiate the polymerization followed by stirring for 2 h at rt to complete the polymerization. The resulting copolymer was purified using a dialysis membrane (Spectrum Laboratories, Inc.; cutoff of 50 kDa) against water for 2 days and confirmed by  $^1\text{H}$  NMR. A series of different PNAP copolymers were synthesized following the same procedure where the NIPAM to AAm molar ratios were varied (3:1, 2.95:1, 2.1:1, 1.25:1).

*Iron Oxide Nanoparticles Coated with Thermoresponsive Polymer (IONPs-PNAP)*

The iron oxide nanoparticles coated with the thermoresponsive polymer were synthesized following the above-described procedure for synthesis of copolymer PNAP in the presence of the TMAOH-stabilized iron oxide nanoparticles. Ten milliliters of Milli-Q water was replaced with 10 mL of magnetic nanoparticles aqueous solution for this synthetic step. The resulting copolymer-coated IONPs were purified using a dialysis membrane (Spectrum Laboratories, Inc.; cutoff of 50 kDa) against water for 2 days. A series of syntheses of copolymer-coated iron oxide nanoparticles were performed to tune the LCST of the resulting nanoparticles with the variation of the NIPAM to AAm ratio (3:1, 2.95:1, 2.1:1, 1.25:1). The concentration of amino groups on the surface was determined by a modified spectrophotometric TNBSA assay as previously described (25). The obtained nanoparticles were lyophilized and kept for further use.

**Characterization of IONPs, PNAP, and IONPs-PNAP***Transmittance Measurements—LCST Determination*

LCST, or cloud point, of the copolymer PNAP and the IONPs-PNAP solutions were evaluated *via* transmittance measurements on a UV-1800 Spectrophotometer (Shimadzu, Carlsbad, CA). The transmittance of a sample is the ratio of the intensity of the light that has passed through the sample to the intensity of the light when it entered the sample. At the LCST, the transmittance of the polymer solution starts to change. Transmittance of the PNAP and the IONPs-PNAP solutions (IONPs concentration 5 mg/mL) was monitored at 700 nm as a function of temperature (with heating/cooling

cycle at 1°C step, cell path length 3 mm) after incubating for 20 min at a defined temperature.

*Size and Zeta Potential Measurements by DLS*

The hydrodynamic size, polydispersity index (PDI), and zeta potential of the prepared nanoparticles were evaluated by dynamic light scattering (DLS) analysis using Malvern ZetaSizer NanoSeries (Malvern Instruments, UK) according to the manufacturer's instructions. Samples were diluted in ultra-pure water, to avoid multiscattering, to the appropriate concentration. The intensity of the He-Ne laser (633 nm) was measured at an angle of 173°. All measurements were performed at 25°C after preequilibration for 2 min, and each parameter was measured in triplicate.

*Transmission Electron Microscopy (TEM)*

The size and morphology of the synthesized iron oxide cores were evaluated using FEI Titan 80–200 TEM/STEM with ChemiSTEM capability (FEI, Hillsboro, OR), operating at 200 kV. One drop of IONPs solution was placed on a copper grid coated with Formvar/carbon film and dried under vacuum. The sizes of the iron oxide cores were obtained after counting over 50 nanoparticles from different TEM images with ImageJ processing software.

*Attenuated Total Reflection Fourier Transform Infrared (ATR-FTIR) Spectroscopy*

Attenuated reflectance infrared spectra of lyophilized samples of IONP-TMAOH, PNAP, and IONPs-PNAP were acquired from a Thermo Electron Corp. Nicolet 6700 FT-IR. The spectra were recorded in the absorbance mode.

*Thermogravimetric Analysis (TGA)*

TGA, providing information about the mass of the sample as a function of temperature, was carried out on the lyophilized sample of IONPs and IONPs-PNAP, from 25°C to 600°C, with a heating rate of 10°C min<sup>-1</sup> using a TGA-1500 thermal gravimetric analyzer (Omnitherm) under nitrogen atmosphere. The amount of IONPs is estimated from the percentage loss of the TGA thermal curve.

*Drug Loading*

The anticancer drug, DOX, was loaded into the thermoresponsive polymer-coated iron oxide nanoparticles IONPs-PNAP in the following manner. In brief, 5 mg of lyophilized nanoparticles was dissolved in 2 mL of water, and 5 mg of DOX was added to the solution followed by vortexing (Vortex Mixer, VWR) for 48 h at rt. The drug-loaded nanoparticles were settled down by using a strong permanent magnet and washed three to four times with water. The residual DOX content was determined by analyzing the obtained supernatant by UV-vis absorption, with a prominent DOX peak appearing around 460 nm over the IONPs background (UV-1800 spectrophotometer, Shimadzu, Carlsbad, CA). The standard curve was generated by measuring DOX absorption intensity at 460 nm in the standard samples containing

different concentrations (from 5 to 100  $\mu\text{g}/\text{mL}$ ) while using a constant concentration of IONPs.

Drug loading efficiency of DOX into the IONPs-PNAP was calculated as follows:

$$\text{Drug loading efficiency}(\%) = W_1 - W_2/W_1 \times 100\%,$$

where  $W_1$  is the total weight of DOX used for drug loading procedure, and  $W_2$  is the weight of DOX present in the supernatant.

#### Drug Release

The drug release profile of DOX from the IONPs-PNAP was evaluated in phosphate-buffered saline (PBS) at pH 7.4. The drug-loaded delivery system was dissolved in 1-mL PBS buffer and placed in a 1-mL Float-A-Lyzer dialysis tubes (molecular weight cutoff of 50 kDa). The dialysis tubes were immersed in 15 mL of PBS buffer and incubated for 96 h at 25 (rt), 37°C (body temperature), and 39°C, the temperature just above the LCST of the corresponding copolymer-coated nanoparticles. At fixed time intervals, 200  $\mu\text{L}$  of the samples were withdrawn from the dialysis tubes to record the absorbance of DOX at 460 nm. After each absorption measurement, the samples were returned to the appropriate dialysis tubes for further incubation. The DOX content in the IONPs-PNAP system at different time points was quantified based on UV-visible absorption spectra with a prominent DOX peak appearing around 460 nm (UV-1800 spectrophotometer, Shimadzu, Carlsbad, CA). The percentage of drug release at different time points was calculated as follows:

$$\text{Drug release}(\%) = [\text{DOX}]_R/[\text{DOX}]_T \times 100\%,$$

where  $[\text{DOX}]_R$  is the amount of DOX released at collection time, and  $[\text{DOX}]_T$  is the total amount of DOX that was encapsulated in the delivery system.

#### In Vitro Study

##### Cell Lines

The A2780/AD multidrug-resistant human ovarian carcinoma cell lines were obtained from T. C. Hamilton (Fox Chase Cancer Center, Philadelphia, PA). Cells were cultured in RPMI 1640 medium (Sigma, St. Louis, MO), supplemented with 10% of fetal bovine serum (VWR, Visalia, CA) and 1.2 mL/100 mL of penicillin-streptomycin (Sigma, St. Louis, MO). Cells were grown at 37°C in a humidified atmosphere of 5%  $\text{CO}_2$  (v/v) in air. All experiments were performed on cells in the exponential growth phase and between passages 2 and 6.

##### Cellular Internalization

Prior to the visualization, A2780/AD cells were plated in a six-well tissue culture plate at a density of  $10 \times 10^3$  cells/well and cultured for 24 h. The medium was then replaced by a suspension of IONPs-PNAP-DOX in the culture media at the concentration of doxorubicin of 5  $\mu\text{g}/\text{mL}$ , and the cells were

incubated for 3 h at 37°C. Cellular internalization of the studied formulations was analyzed by a fluorescence microscope (Leica Microsystems Inc., Buffalo Grove, IL).

#### Cytotoxicity Studies

The cellular cytotoxicity of all studied formulations was assessed using a modified Calcein AM cell viability assay (Fisher Scientific Inc.). Briefly, cancer cells were seeded into 96-well microtiter plates at the density of  $10 \times 10^3$  cells/well and allowed to grow for 24 h at 37°C, and at the temperature just above the LCST of the corresponding copolymer-coated nanoparticles, respectively. Then the culture medium was discarded and the cells were treated for 24 h with 200  $\mu\text{L}$  of medium containing different concentrations of the following formulations: (1) control (cell only in fresh media), (2) IONPs-PNAP (IONPs content from 1 to 550  $\mu\text{g}/\text{mL}$ ), and (3) IONPs-PNAP-DOX (IONPs content from 1.0 to 550  $\mu\text{g}/\text{mL}$  and DOX concentration from 0.50 to 250  $\mu\text{g}/\text{mL}$ ). After treatment, the cells were rinsed with Dulbecco's phosphate-buffered saline (DPBS) buffer and incubated for 1 h with 200  $\mu\text{L}$  of freshly prepared Calcein AM solution (10  $\mu\text{M}$  in DPBS buffer). Fluorescence was measured using a multiwell plate reader (Synergy HT, BioTek Instruments, Winooski, VT) with a 485-nm excitation and 528-nm emission filters. On the basis of these measurements, cellular viability was calculated for each concentration of the formulation tested. The relative cell viability (%) was expressed as a percentage relative to the untreated control cells.

## RESULT AND DISCUSSION

### Iron Oxide Nanoparticles Coated with Thermoresponsive Copolymer

In order to develop the thermoresponsive nanosystem for effective delivery and temperature-triggered drug release, water-soluble IONPs-TMAOH have been synthesized by coprecipitation of Fe(II) and Fe(III) chlorides with 0.5  $\text{Fe}^{\text{II}}/\text{Fe}^{\text{III}}$  ratio using 1.5 M of NaOH as a reducing agent. The dark brown precipitate was collected on a magnet, washed with water, and incubated with 0.1 M TMAOH to prevent aggregation of the IONPs. The prepared IONPs were stable in water for 4 weeks at room temperature due to the TMAOH modification. DLS analysis revealed that the stabilized nanoparticles with TMAOH have a hydrodynamic size of  $99.8 \pm 0.3$  nm (Table I) which is about 85 nm larger than the iron oxide core size measured by TEM ( $12.2 \pm 1.75$ , Fig. 2). This is due to the fact that in our experiment, TEM permits only the observation of the size of the iron oxide core and estimates its real diameter, while DLS gives us the ability to evaluate the hydrodynamic diameter of nanoparticles, which takes into accounts the surfactant and interaction with the solvent molecules. The polydispersity index (PDI) of  $0.141 \pm 0.010$  indicates stability and a narrow size distribution of IONPs (Table I). The zeta potential of the prepared IONPs was highly negative  $-45.0 \pm 1.7$  mV (Table I), which is attributed to the presence of  $\text{OH}^-$  groups on the surface of the IONPs after TMAOH stabilization (Fig. 1).

**Table I.** Characterization of IONPs Stabilized with TMAOH, Modified with Copolymer PNAP, and Loaded with DOX

	Size, nm (DLS)	PDI	Zeta potential, mV	DOX loading, %
IONPs-TMAOH	99.8±0.3	0.141±0.010	-45.0±1.7	-
IONPs-PNAP	130.1±0.2	0.180±0.010	+18.0±1.5	-
IONPs-PANP-DOX	139.7±0.7	0.129±0.013	+21.6±0.7	44.5

*DLS* dynamic light scattering, *PDI* polydispersity index, *DOX* doxorubicin, *IONPs-TMAOH* tetramethylammonium hydroxide pentahydrate-stabilized iron oxide nanoparticles, *IONPs-PNAP* iron oxide nanoparticles coated with thermoresponsive polymer, *IONPs-PANP-DOX* DOX-loaded iron oxide nanoparticles coated with thermoresponsive polymer

To impart the temperature-triggered drug release capability to the iron oxide nanoparticles, a PNIPAM-based thermoresponsive copolymer has been employed for surface modification of the nanoparticles. PNIPAM is known to undergo rapid and reversible hydrophilic to hydrophobic phase transition around 32°C (LCST or cloud point) due to the dual nature of PNIPAM containing both a hydrophilic amide group and a hydrophobic isopropyl group (26). Below the LCST, PNIPAM becomes hydrated with expanded structure and

completely soluble in water due to the hydrogen bonds offering easy drug loading. Above the LCST, the weak H-bonds in PNIPAM break and hydrophobic functional groups become dominant, and hence, the polymer becomes insoluble in water collapsing into tightly packed globular conformation causing the drug release. To achieve temperature-triggered drug release specifically in tumors ( $T > 37^\circ\text{C}$ ) after the application of external heat while trying to avoid drug leakage from the delivery system during systemic circulation ( $T = 37^\circ\text{C}$ ), the LCST of PNIPAM has to be increased from 32°C to an LCST above body temperature. Thus, LCST of the polymer can be adjusted upon shifting hydrophobic/hydrophilic balance in the PNIPAM molecular structure (5). Hence, hydrophilic monomer, acrylamide (AAM), known to increase the transition temperature of PNIPAM, was incorporated into the copolymer to tune its LCST. Additionally, cationic PEI provided the positive charges to the synthesized copolymer required for the further electrostatic absorption of the final copolymer on negatively charged IONPs-TMAOH. To tune the LCST to the required values, the copolymer poly-(NIPAM-AAM)-PEI (PNAP) was synthesized at various NIPAM:AAM ratios (3:1, 2.95:1, 2.1:1, 1.25:1), and, as depicted in Fig. 3a (black line), the cloud point of the copolymer increases with the decrease of the content of NIPAM in the feed. Higher concentration of the hydrophobic functional groups introduced by NIPAM cause the copolymer to reach the LCST earlier than the copolymer having less-hydrophobic functional groups. The solutions are homogeneous at  $T < \text{LCST}$ , and a phase separation occurs when the temperature exceeds the LCST resulting in the decreased transmittance (Fig. 3b). The transmittance *versus* temperature plot (Fig. 4a) indicates that the phase transition of prepared PNAP is reversible within several degrees upon cooling and heating. Thus, the composition of the copolymer could be adjusted to tune the LCST, specifically between 38°C and 44°C for the temperature-controlled drug release.

Next, the cationic PNAP was introduced onto the anionic surface of IONPs through strong ionic interactions. This modification was achieved *via* the above-described copolymerization process in the presence of IONPs (Fig. 1a). The iron oxide nanoparticles coated with the PNAP (IONPs-PNAP) were synthesized using the same ratios of the NIPAM:AAM as for the above-described synthesized thermoresponsive copolymer. The presence of the iron oxide nanoparticle influenced the LCST of the resulting IONPs coated with poly-(NIPAM-AAM)-PEI complex by 1°C–2°C (Fig. 3a, red line). Thus, these studies reveal that the LCST of the IONPs-PNAP nanoparticles can be tuned by changing the NIPAM:AAM molar ratio during copolymerization process on the nanoparticle surface. In addition, the ratio between the IONPs and copolymer should be taken

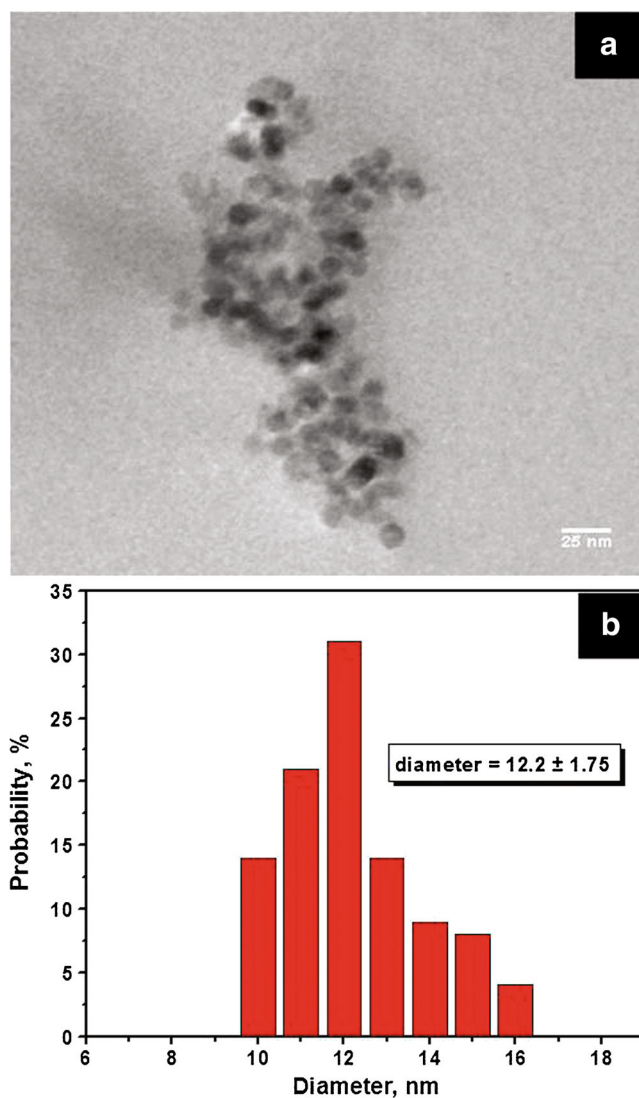


**Fig. 2.** A representative TEM image of iron oxide nanoparticles **a** and the size distribution of the corresponding particles **b**

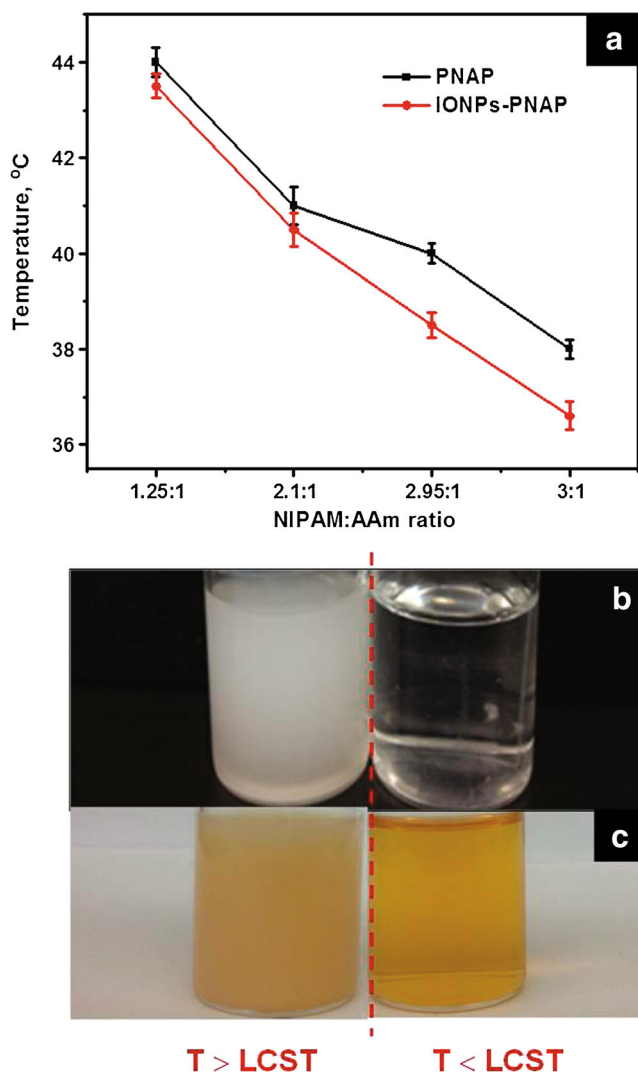


**Fig. 3.** **a** The lower critical solution temperature (LCST) of thermoresponsive PNAP copolymer alone (black line) and coated onto the IONPs surface (red line). On the right, images show visual evidence of the thermoresponsive behavior of PNAP copolymer **b** and the IONPs coated with the PNAP **c** above and below the LCST

into consideration for preparation of the drug delivery system with desired LCST. The drastic decrease in transmittance of the clear aqueous solution of IONPs-PNAP was observed with the increasing temperature above the LCST (Fig. 3c). The sharp transition curves were recorded for all four tested copolymers with various NIPAM:AAM ratios (Fig. 4b), indicating LCST behavior. It must be noted that no significant changes in the LCST behavior were observed within 1–20 mg/mL concentration range for all four studied IONPs-PNAP systems (data not shown).

The IONPs coated with the copolymer prepared at the NIPAM:AAM ratio of 2.95:1 demonstrated the transition temperature, 38°C–39°C, just above the body temperature (Fig. 3a, red line), which is the most desirable property for the development of the effective temperature-triggered “on-off” drug delivery system. The above-described IONPs were employed for further studies. DLS analysis of the IONPs-PNAP detected a 30 nm increase in particle size after the copolymer coating onto IONPs showing the hydrodynamic

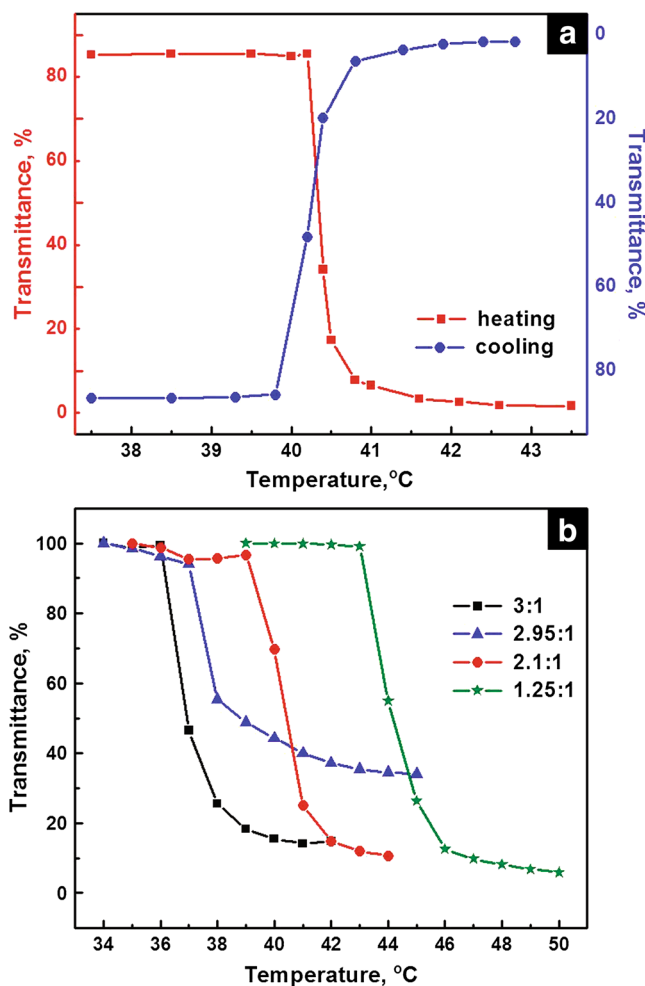


**Fig. 4.** **a** The transmittance versus temperature plot for copolymer PNAP (NIPAM:AAM 2.95:1) indicating reversible behavior. **b** The transmittance versus temperature plots for the IONPs-PNAP with various the NIPAM to AAM ratio

size of  $130.1 \pm 0.2$  nm, with the polydispersity index (PDI) of  $0.180 \pm 0.010$  (Table I). Thus, the final nanocarriers have a hydrodynamic size within the desired range of 10–200 nm to prevent elimination by the kidneys (<10 nm) and recognition by macrophage cells (>150 nm) and enhance tumor-targeted delivery *via* EPR effect (<200 nm). The zeta potential of the IONPs modified with PNAP became positive ( $+18.0 \pm 1.5$  mV, Table I) due to the presence of protonated amino groups of PEI on the IONPs surface. The excess of amino groups of PEI on the nanoparticle surface was confirmed by TNBSA assay and can provide the possibility of further desired functionalization of the delivery system with cancer targeting moieties.

#### ATR-FTIR

Further evidence of the successful preparation of the copolymer-coated IONPs is provided by ATR-FTIR spectra as shown in Fig. 5a, along with the spectra of the IONPs stabilized with TMAOH and the PNAP copolymer as a reference. The ATR-FTIR spectrum of the IONPs-PNAP exhibited the characteristic absorption bands of poly-(NIPAM-stat-AAm)-block-PEI. The absorption peak at  $\sim 3,500$ – $3,100$   $\text{cm}^{-1}$

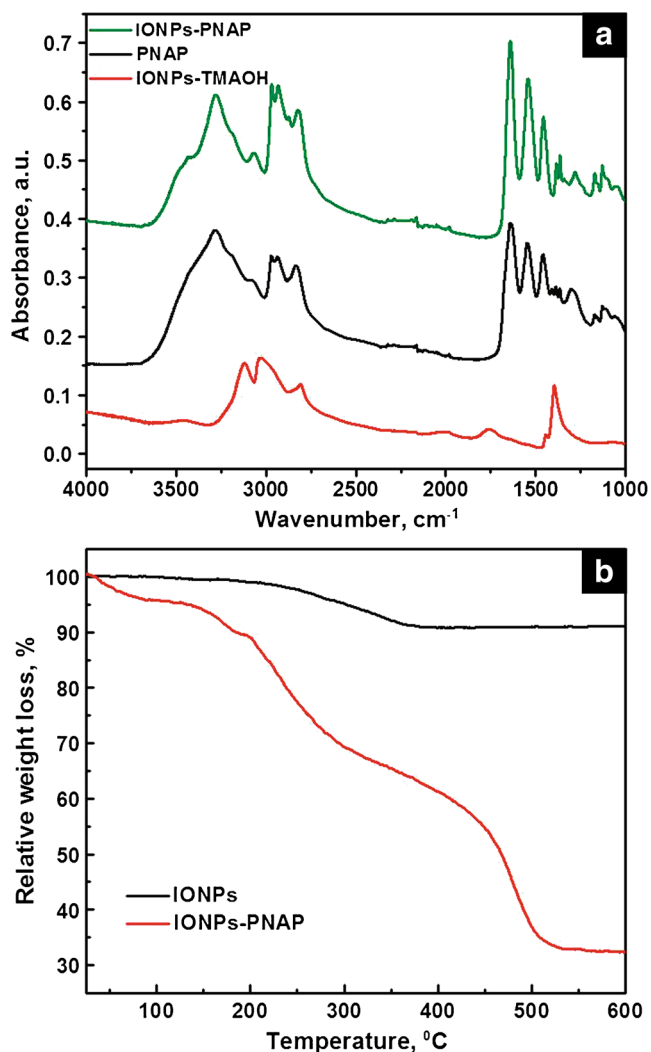


**Fig. 5.** **a** ATR-FTIR spectra of the IONPs stabilized with TMAOH (red line), the thermoresponsive copolymer PNAP (black line), and the IONP-PNAP (green line). **b** TGA analysis of the IONPs (black line) and the IONPs-PNAP (red line)

can be attributed to the stretch of the  $\text{NH}_2$  and  $\text{NH}$  groups of copolymer. A small peak around  $3440\text{ cm}^{-1}$  in the IONPs-PNAP sample corresponds to the primary amine of PEI which became more distinguished on the IONPs surface compared to the secondary amine of NIPAM. The asymmetric stretching vibration of the alkyl groups occurs at  $\sim 2,950\text{--}2,850\text{ cm}^{-1}$ ; the secondary amide  $\text{C}=\text{O}$  stretching in NIPAM and AAm shows a strong band at  $1,650\text{ cm}^{-1}$ ; and the asymmetric bending deformation of  $\text{N-H}$  and alkyl groups occurs at  $1,550$  and  $1,450\text{ cm}^{-1}$ , respectively.

### Thermogravimetric Analysis (TGA)

TGA was carried out to confirm the copolymerization on the surface of the IONPs and estimate the relative composition of the thermoresponsive copolymer and iron oxide nanoparticles where the mass of a substance is monitored as a function of temperature. Figure 5b shows TGA thermal curves of IONPs and IONPs-PNAP. As expected, the TGA curve for IONPs shows almost no significant weight loss due

to thermal stability of the iron oxide in the employed temperature range. The observed slight weight loss in the sample of IONP is attributed to the evaporation of residual water and possible TMAOH loss after  $300^\circ\text{C}$ . The TGA thermal curve for the nanoparticle-PNAP system revealed a four-step weight loss. The initial weight loss around  $100^\circ\text{C}$  was due to the evaporation of moisture embedded in the sample which is not significant in comparison to the weight loss attributed to the decomposition of the copolymer in the subsequent steps. The following weight reduction corresponds to the step by step removal of NIPAM, AAm, and PEI resulting in the significant weight loss of  $\sim 80\%$  between  $125^\circ\text{C}$  and  $525^\circ\text{C}$ . This indicates the presence of  $\sim 80\%$  of copolymer on the IONP surface. There was no significant weight change after  $525^\circ\text{C}$ , implying the presence of iron oxide only. Thus, it could be concluded that the thermoresponsive polymer-coated iron oxide nanoparticles consist of  $\sim 20\%$  of IONPs.

### Drug Loading Efficiency and Temperature-Triggered Drug Release

We tested doxorubicin (DOX) as a drug candidate for our newly developed drug carrier with temperature-controlled release capability. DOX, being one of the most widely used chemotherapeutic anticancer drugs, however, causes serious side effects presenting high systemic toxicity to healthy tissue (27). Effective encapsulation of DOX into nontoxic thermoresponsive IONPs-based delivery vehicle offers a temperature-triggered drug release while reducing the free DOX concentration during the systemic circulation and thus minimizing cytotoxicity of the chemotherapeutic agent to the healthy organs (28). Recently, encapsulation of drugs into iron oxide nanoparticles has shown promise for overcoming multidrug resistance (29). In comparison to the covalent conjugation, physical loading of DOX in the polymer surface layer offers to preserve the therapeutic efficacy of the drug (30,31). Hence, our drug loading approach is based on the availability of a drug reservoir formed by copolymer chains on the developed IONPs surfaces. We found that DOX can be efficiently incorporated into the copolymer layers on IONPs surfaces by vigorous mixing of the IONPs with the appropriate amount of the drug in water at room temperature. Thus, a DOX to IONPs ratio of 5 mg of DOX: 5 mg of IONPs-PNAP resulted in the drug loading efficiency to be as high as 44.5% w/w. Drug loading efficiency was strongly dependent on the DOX concentration during the drug loading process for the same type of IONPs-PNAP and decreases as the DOX:IONPs ratio reduced (data not shown). The 1:1 ratio of DOX:IONPs-PNAP resulted in the highest drug loading efficiency and was used for further studies. Next, examining the hydrodynamic size of the DOX-loaded IONPs, we observed that the resulting iron oxide nanoparticles loaded with DOX are  $139.7 \pm 0.7\text{ nm}$  in diameter with uniform size distribution ( $\text{PDI } 0.129 \pm 0.013$ ), which is larger than IONPs-PNAP alone ( $130.1 \pm 0.2\text{ nm}$ , Table I). An increase in nanoparticles size can be attributed to the swelling of polymer coating on the nanoparticles surface upon DOX encapsulation as was previously reported (32). In contrast, the zeta potential values of the prepared IONPs ( $+18.0 \pm 1.5$ ) were not affected by the encapsulation of DOX ( $+21.6 \pm 0.7$ , Table I). The data suggest that DOX is not

physically adsorbed on IONPs but rather encapsulated into the polymer coating of iron oxide nanoparticles.

Another critical aspect for the development of an effective drug delivery system is the ability of the drug to be released from the carrier at the diseased site and not during the transportation process. Due to the temperature-sensitive coil-to-globule transition behavior of PNIPAM-based copolymer at the LCST, the on-off dissociation of drug molecules as a function of temperature is expected. To assess the potential of the developed delivery system as a drug carrier capable of triggered drug release, the release profiles of DOX from IONPs-PNAP were evaluated in PBS buffer at 7.4 (pH of blood plasma) at 25 (room temperature), 37°C (body temperature), and 39°C, the temperature just above the LCST of IONPs-PNAP (Fig. 6). We detected an initial DOX

release of 10% within the first 4 h of IONPs-PNAP incubation at pH 7.4 at ~39°C. Further incubation of the delivery system for 92 h under the same experimental conditions resulted in 45% of total drug release. In contrast, only ~7% and 10% of the total DOX was gradually released at pH 7.4 after 96 h of incubation at 25°C and 37°C, respectively. The faster drug release at 39°C can be attributed to the fast polymer collapse leading to the rapid expulsion of water together with the drug. The difference in release kinetics at 37°C and 39°C indicated that the developed drug delivery system shows temperature-dependent drug release behavior. Such behavior is important for the development of an effective and nontoxic drug delivery system because it ensures a very low drug release at the physiological pH 7.4 at 37°C during the transport of the drug in the blood stream (31,33,34). On the other hand, the IONPs-PNAP are capable of the temperature-triggered release above its LCST.

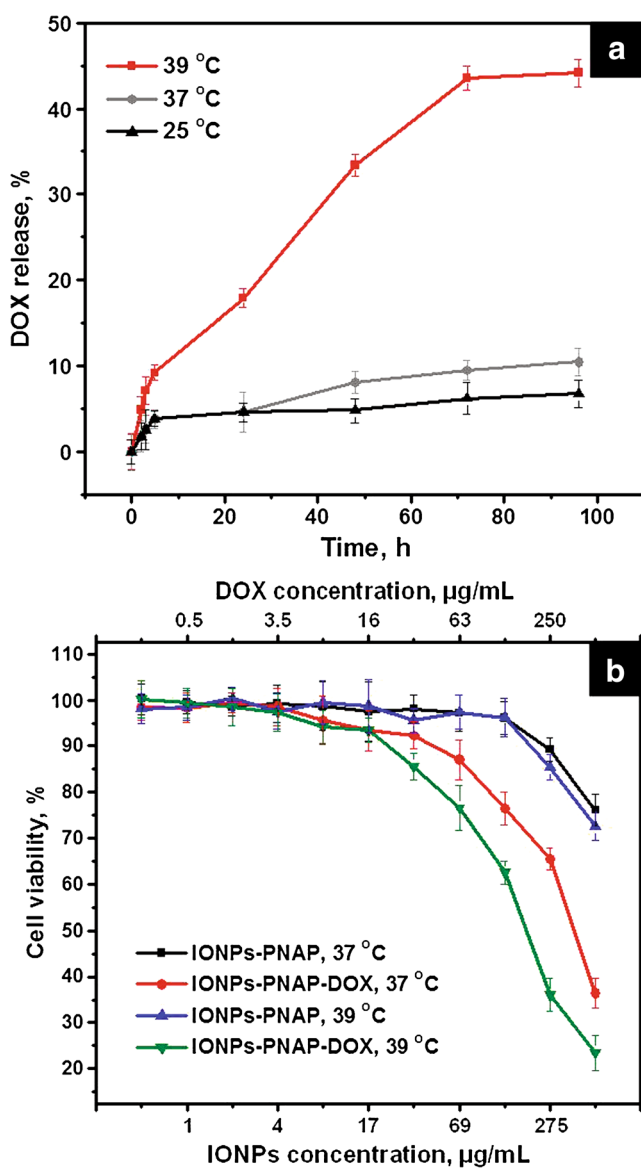


**Fig. 6.** **a** The release profiles of DOX from IONPs-PNAP-DOX incubated at 25°C, 37°C, and 39°C (temperature just above the LCST of the copolymer with the NIPAM:AAM ratio of 2.95:1) in PBS buffer at pH 7.4. **b** *In vitro* cytotoxicity at 37°C and 39°C of IONPs-PNAP (black and blue lines) and the DOX-loaded IONPs-PNAP system (IONPs-PNAP-DOX, red and green lines) against A2780/AD human ovarian cancer cells after 24 h of incubation

### *In Vitro* Studies

The intracellular localization of DOX plays an important role in its anticancer activity (34,35). Therefore, localization of DOX in the multidrug-resistant A2780/AD ovarian carcinoma cells after incubation with drug loaded into IONPs-PNAP was evaluated by fluorescence microscopy employing intrinsic fluorescence properties of DOX. We found that DOX delivered by IONPs-PNAP was predominantly distributed in the cytoplasm after 3 h of incubation (Fig. 7). The DOX-loaded nanoparticles are expected to be taken up by cancer cells *via* endocytosis, followed by endosomal/lysosomal escape and drug release in the cytoplasm followed by drug diffusion to the nucleus (34). It is also very important to evaluate the

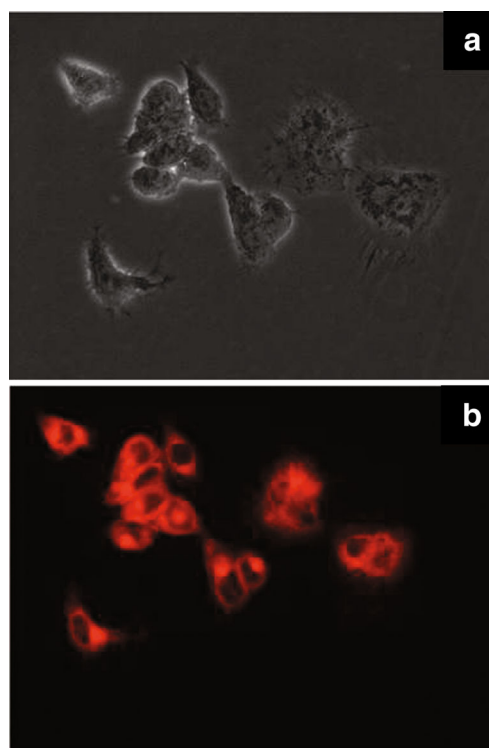


**Fig. 7.** Representative light **a** and fluorescence **a** microscopy images demonstrate intracellular localization of DOX in A2780/AD cancer cells after incubation with the IONPs-PNAP-DOX for 3 h



biocompatibility of the IONPs-PNAP for the actual application in drug delivery. Thus, the drug-free IONPs-PNAP were found to be nontoxic toward A2780/AD cells with the cell viability of 80%–100% at the concentrations of the IONPs-PNAP from 1.0 to 550  $\mu\text{g}/\text{mL}$  (Fig. 6b) at both 37°C (body temperature) and 39°C (just above the LCST of the IONPs-PNAP with the NIPAM:AAM ratio of 2.95:1). However, when the nanoparticles were loaded with DOX, the sufficient decrease in cell viability was observed after incubation for 24 h at 39°C as compared to the treatment at 37°C (Fig. 6b). This indicates an improved DOX release above the LCST of the developed drug carrier and its thermoresponsive properties needed for the temperature-triggered drug release. Thus, the IONPs-PNAP delivery system reduced the amount of available drug in the extracellular environment that will potentially diminish unwanted side-target effects on healthy organs *in vivo* and inhibits multidrug resistance as compared to free DOX (34).

To investigate in more details the influence of IONPs-PNAP loaded with DOX on ovarian cancer cells, we studied cell growth of A2780/AD after treatment by BrdU proliferation assay (Fig. S1). Proliferation of ovarian cancer cell treated with IONPs-PNAP-DOX was decreased in the 40°C treatment group compared to the 37°C confirming the temperature conformational change of the PNAP causing the enhanced DOX release into the cytoplasm. Next, additional cytotoxicity studies were performed by measuring plasma membrane damage based on the release of lactate dehydrogenase (LDH). The LDH assay shows a slight increase in cytotoxicity of the 37°C treatment group *versus* the 39°C possibly attributing the increase in cytotoxicity to mild hyperthermia (Fig. S2). The influence of IONPs-PNAP loaded with DOX on the intracellular reactive oxygen species (ROS) level of A2780/AD cells was evaluated by H2DCFDA assay and compared to the ROS generation of nontreated cells and cells treated with DOX only at the same DOX concentration (Fig. S3). The data for all treated and control groups demonstrated similar ROS level, suggesting that ROS is probably not the mechanism by which cytotoxicity is conferred.

## CONCLUSIONS

In this study, a two-step modification approach was successfully employed to develop the temperature-tunable iron oxide nanoparticles with a biocompatible and thermoresponsive polymeric shell consisting of the poly-(NIPAM-stat-AAm)-block-PEI block copolymer. Varying the copolymer composition and the IONPs to copolymer ratio allows the adjustment of the phase transition temperature of the IONPs-PNAP between 36°C and 44°C. The size of IONPs-PNAP system was found to be within the desired range of 10–150 nm for the effective drug delivery of the nanosystems. ATR-FTIR and a quantitative analysis of the polymeric content obtained by thermogravimetric analysis confirmed the modification of IONPs with the thermoresponsive copolymer. A maximum DOX loading into the IONPs-PNAP of ~45% was obtained. Release rates of the DOX from the IONPs-PNAP under different temperatures revealed the thermoresponsive properties of the IONPs-based platform. An improved release of DOX and anticancer efficacy was achieved at the temperature a few degrees higher than body temperature. Notably, the LCST of the IONPs-PNAP is

reversible and not concentration dependent. High stability under physiological conditions and low toxicity together with their temperature-tunable properties and their ease of preparation make the developed IONPs-based platform an attractive candidate for drug delivery with remote-controlled drug release.

## ACKNOWLEDGMENTS

This work was supported in part by the funding provided by the Medical Research Foundation of Oregon, PhRMA Foundation and the College of Pharmacy, Oregon State University. We thank Teresa Sawyer (Electron Microscopy Facility, OSU) for TEM analysis and Dr. Christine Pastorek (Department of Chemistry, OSU) for access to the FTIR-ATR and TGA instruments.

## REFERENCES

1. Lopes J, Santos G, Barata P, Oliveira R, Lopes CM. Physical and chemical stimuli-responsive drug delivery systems: targeted delivery and main routes of administration. *Curr Pharm Des.* 2013;Epub ahead of print.
2. Alexander C, Shakesheff KM. Responsive polymers at the biology/materials science interface. *Adv Mater.* 2006;18:3321–8.
3. Allen TM, Cullis PR. Drug delivery systems: entering the mainstream. *Science.* 2004;303:1818–22.
4. Cheng R, Meng FH, Deng C, Klok HA, Zhong ZY. Dual and multi-stimuli responsive polymeric nanoparticles for programmed site-specific drug delivery. *Biomaterials.* 2013;34:3647–57.
5. Schmaljohann D. Thermo- and pH-responsive polymers in drug delivery. *Adv Drug Deliv Rev.* 2006;58:1655–70.
6. Muller-Schulte D, Schmitz-Rode T. Thermosensitive magnetic polymer particles as contactless controllable drug carriers. *J Magn Magn Mater.* 2006;302:267–71.
7. Eeckman F, Moes AJ, Amighi K. Synthesis and characterization of thermosensitive copolymers for oral controlled drug delivery. *Eur Polymer J.* 2004;40:873–81.
8. Laurent S, Dutz S, Hafeli UO, Mahmoudi M. Magnetic fluid hyperthermia: focus on superparamagnetic iron oxide nanoparticles. *Adv Colloid Interface Sci.* 2011;166:8–23.
9. Liu XQ, Kaminski MD, Chen HT, Torno M, Taylor L, Rosengart AJ. Synthesis and characterization of highly-magnetic biodegradable poly(D, L-lactide-co-glycolide) nanospheres. *J Control Release.* 2007;119:52–8.
10. Laurent S, Mahmoudi M. Superparamagnetic iron oxide nanoparticles: promises for diagnosis and treatment of cancer. *Int J Mol Epidemiol Genet.* 2011;2:367–90.
11. Vihola H, Laukkanen A, Valtola L, Tenhu H, Hirvonen J. Cytotoxicity of thermosensitive polymers poly(*N*-isopropylacrylamide), poly(*N*-vinylcaprolactam) and amphiphilically modified poly(*N*-vinylcaprolactam). *Biomaterials.* 2005;26:3055–66.
12. Kuckling D, Adler HJP, Arndt KF, Ling L, Habicher WD. Temperature and pH dependent solubility of novel poly(*N*-isopropylacrylamide) copolymers. *Macromol Chem Phys.* 2000;201:273–80.
13. Principi T, Goh CCE, Liu RCW, Winnik FM. Solution properties of hydrophobically modified copolymers of *N*-isopropylacrylamide and *N*-glycine acrylamide: a study by microcalorimetry and fluorescence spectroscopy. *Macromolecules.* 2000;33:2958–66.
14. Hoogenboom R, Thijs HML, Jochems MJHC, Lankvelt BM, Fijten MWM, Schubert US. Tuning the LCST of poly(2-oxazoline)s by varying composition and molecular weight: alternatives to poly(*N*-isopropylacrylamide). *Chem Comm.* 2008;5758–60.
15. Zintchenko A, Ogris M, Wagner E. Temperature dependent gene expression induced by PNIPAM-based copolymers: potential of hyperthermia in gene transfer. *Bioconj Chem.* 2006;17:766–72.

16. Narain R, Gonzales M, Hoffman AS, Stayton PS, Krishnan KM. Synthesis of monodisperse biotinylated p(NIPAAm)-coated iron oxide magnetic nanoparticles and their bioconjugation to streptavidin. *Langmuir*. 2007;23:6299–304.
17. Deng Y, Yang W-L, Wang C, Fu S. A novel approach for preparation of thermoresponsive polymer magnetic microspheres with core-structure. *Adv Mater*. 2003;15:1729–32.
18. Zhang S, Zhang L, He B, Wu Z. Preparation and characterization of thermosensitive PNIPAA-coated iron oxide nanoparticles. *Nanotechnology*. 2008;19:325608.
19. Zhang JL, Srivastava RS, Misra RDK. Core-shell magnetite nanoparticles surface encapsulated with smart stimuli-responsive polymer: synthesis, characterization, and LCST of viable drug-targeting delivery system. *Langmuir*. 2007;23:6342–51.
20. Liu G, Hu D, Chen M, Wang CC, Wu LM. Multifunctional PNIPAM/Fe<sub>3</sub>O<sub>4</sub>-ZnS hybrid hollow spheres: synthesis, characterization, and properties. *J Colloid Interface Sci*. 2013;397:73–9.
21. Hao L, Yang H, Lei ZL. Synthesis and properties of thermoresponsive macroporous PAM-co-PNIPAM microspheres. *Mater Lett*. 2012;70:83–5.
22. Talelli M, Rijcken CJF, Lammers T, Seevinck PR, Storm G, van Nostrum CF, *et al.* Superparamagnetic iron oxide nanoparticles encapsulated in biodegradable thermosensitive polymeric micelles: toward a targeted nanomedicine suitable for image-guided drug delivery. *Langmuir*. 2009;25:2060–7.
23. Gaharwar AK, Wong JE, Muller-Schulte D, Bahadur D, Richtering W. Magnetic nanoparticles encapsulated within a thermoresponsive polymer. *J Nanosci Nanotechnol*. 2009;9:5355–61.
24. Lyon JL, Fleming DA, Stone MB, Schiffer P, Williams ME. Synthesis of Fe oxide core/Au shell nanoparticles by iterative hydroxylamine seeding. *Nano Lett*. 2004;4:719–23.
25. Taratula O, Garbuzenko OB, Kirkpatrick P, Pandya I, Savla R, Pozharov VP, *et al.* Surface-engineered targeted PPI dendrimer for efficient intracellular and intratumoral siRNA delivery. *J Control Release*. 2009;140:284–93.
26. Jun L, Bochu W, Yazhou W. Thermo-sensitive polymers for controlled-release drug delivery systems. *Int J Pharmacol*. 2006;2:513–9.
27. Tacar O, Sriamornsak P, Dass CR. Doxorubicin: an update on anticancer molecular action, toxicity and novel drug delivery systems. *J Pharm Pharmacol*. 2013;65:157–70.
28. Peng XH, Qian XM, Mao H, Wang AY, Chen Z, Nie SM, *et al.* Targeted magnetic iron oxide nanoparticles for tumor imaging and therapy. *Int J Nanomedicine*. 2008;3:311–21.
29. Kievit FM, Wang FY, Fang C, Mok H, Wang K, Silber JR, *et al.* Doxorubicin loaded iron oxide nanoparticles overcome multidrug resistance in cancer in vitro. *J Control Release*. 2011;152:76–83.
30. Quan QM, Xie J, Gao HK, Yang M, Zhang F, Liu G, *et al.* HSA coated iron oxide nanoparticles as drug delivery vehicles for cancer therapy. *Mol Pharm*. 2011;8:1669–76.
31. Yang LL, Cao ZH, Sajja HK, Mao H, Wang LY, Geng HY, *et al.* Development of receptor targeted magnetic iron oxide nanoparticles for efficient drug delivery and tumor imaging. *J Biomed Nanotechnol*. 2008;4:439–49.
32. Taratula O, Dani RK, Schumann C, Xu H, Wang A, Song H, *et al.* Multifunctional nanomedicine platform for concurrent delivery of chemotherapeutic drugs and mild hyperthermia to ovarian cancer cells. *Int J Pharm*. 2013;458:169–80.
33. Hruby M, Konak C, Ulbrich K. Polymeric micellar pH-sensitive drug delivery system for doxorubicin. *J Control Release*. 2005;103:137–48.
34. MacKay JA, Chen MN, McDaniel JR, Liu WG, Simnick AJ, Chilkoti A. Self-assembling chimeric polypeptide-doxorubicin conjugate nanoparticles that abolish tumours after a single injection. *Nat Mater*. 2009;8:993–9.
35. Shi M, Ho K, Keating A, Shoichet MS. Doxorubicin-conjugated immuno-nanoparticles for intracellular anticancer drug delivery. *Adv Funct Mater*. 2009;19:1689–96.